Journal of Electrostatics xxx (2016) 1–5

Contents lists available at ScienceDirect

Journal of Electrostatics

journal homepage: www.elsevier.com/locate/elstat

Impact of the laminar flow on the electrical double layer development

P. Leblanc [a, *], J.M. Cabaleiro [b], T. Paillat [a], G. Touchard [a]

[a] Institut Pprime, CNRS–Université de Poitiers – ISAE-ENSMA, 86962 Futuroscope Chasseneuil, France
[b] CONICET-Laboratorio de Fluidodinámica-UBA, and Laboratorio de Micro y Nanofluídica y Plasma, UdeMM, Buenos Aires, Argentina

ARTICLE INFO

Article history:
Received 14 October 2016
Received in revised form
22 November 2016
Accepted 30 November 2016
Available online xxx

Keywords:
Electrical double layer theory
Numerical simulation
Chemical reaction rate
Flow electrification

ABSTRACT

As soon as a liquid comes into contact with a solid, physicochemical reactions occur at the solid-liquid interface to form an electrical double layer. According to the classical theory, it is assumed that the laminar flow has no impact on the global rate of the physicochemical reactions (K_f). However, recent studies have shown that this assumption is not consistent with the experimental results. It seems that K_f is impacted by the flow velocity of the liquid. The aim of this work is to compare the experimental behavior with the numerical simulation taking this variation into account.

© 2016 Elsevier B.V. All rights reserved.

1. Introduction

The flow electrification phenomenon has been studied for a long time [1–3]. Basically, in the dielectric liquid, impurities are assumed to be responsible of the electrical double layer's (EDL) development at the solid-liquid interface. The interface becomes polarized with two opposite charge layers: one inside the liquid and the other within the solid. When a liquid flow is induced, part of the charge inside the liquid is swept, leading to the flow electrification phenomenon. Indeed, the chemical imbalance caused by the flow triggers the creation of new electrical charges within the dielectric liquid (Q_L) and opposite charges in the solid (Q_S). However, the physicochemical reactions at the origin of the EDL are still poorly understood. Most models proposing a better understanding of this phenomenon, such as the adsorption model [4], the corrosion model [5] or a combination of both [6], assume that the global rate of this physicochemical reaction K_f is independent of the flow parameters. However, recent studies [7–9] have shown that this assumption is not consistent with the experimental results.

Using the finite volume CFD tool Code-Saturne® from EDF (Electricité de France), a module has been developed in order to simulate an adsorption model. The equations of this model [10] are coupled to the Navier-Stokes equation. This work presents a numerical analysis between both cases (K_f constant and variable) based on the experimental results. The simulation was carried out using the variation of K_f as a function of the mean velocity observed during the experimental campaign on the flow electrification of mineral oil through a stainless steel duct [8].

2. Adsorption model

2.1. Scheme of the physicochemical adsorption model

The model assumes that the neutral impurities present within the liquid are dissociated in two ionic species: positive and negative. In the case where only one type of impurities reacts at the solid-liquid interface, the chemical reaction is given as follows:

$$A_L B_L \underset{k_r^L}{\overset{k_d^L}{\rightleftharpoons}} A_L^+ + B_L^- \quad (1)$$

where k_d^L and k_r^L are the kinetic constants of the dissociation/recombination reactions. Before the liquid comes into contact with the solid, the liquid and the solid are electrically neutral. The ionic species may react according to the adsorption model (Fig. 1).

Close to the interface, the solid medium is composed of many preferential adsorption sites. Thus, this model assumes that the negative ionic chemical species B_L^- are adsorbed at the solid surface by these sites, called C_S, to form the occupied site $C_S B_L^-$:

* Corresponding author.
E-mail address: paul.leblanc@univ-poitiers.fr (P. Leblanc).

http://dx.doi.org/10.1016/j.elstat.2016.11.006
0304-3886/© 2016 Elsevier B.V. All rights reserved.

Please cite this article in press as: P. Leblanc, et al., Impact of the laminar flow on the electrical double layer development, Journal of Electrostatics (2016), http://dx.doi.org/10.1016/j.elstat.2016.11.006

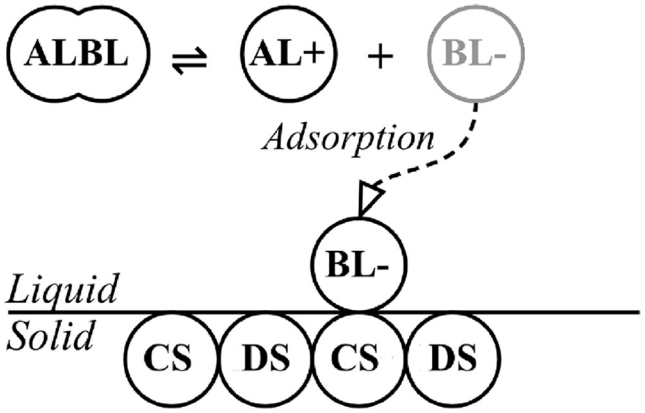

Fig. 1. Scheme of the physicochemical mechanism occurring at the solid-liquid interface for the adsorption hypothesis.

$$C_S + B_L^- \underset{k_{rn}}{\overset{k_{fn}}{\rightleftharpoons}} C_S B_L^- \tag{2}$$

where k_{fn} and k_{rn} represent rates of negative adsorption and desorption, respectively. As in the majority of situations observed within experiments, in this model, the liquid is charged positively and the solid is negatively.

2.2. Electric charge transport mechanisms

All the chemical species, positive (P), negative (N) and neutral (O) are transported within the liquid by three mechanisms: diffusion (Diff.), migration (Mig.) and convection (Conv., when the liquid flow is induced). The flux density can be expressed with the charge species "i" in the liquid (L) as:

$$\overrightarrow{\Gamma_i^L} = -\overbrace{D_i^L \nabla n_i}^{Diff.} \pm \overbrace{n_i \frac{e_0 z_i D_i^L}{kT} \nabla \varphi}^{Mig.} + \overbrace{n_i \overrightarrow{u}}^{Conv.} \quad {}^{Conv.} \tag{3}$$

where,

The general conservation equation can be expressed as follows:

$$\frac{\partial n_i}{\partial t} + \nabla \cdot \overrightarrow{\Gamma_i^L} = G_i - R_i \tag{4}$$

where G_i and R_i represent the generation and recombination species due to the chemical reactions. For example, the chemical reactions of B_L^- within the liquid can be expressed in more explicit forms:

$\overrightarrow{\Gamma_i^L}$	Ionic flux density vector ($m^2 \cdot s^{-1}$)
D_i^L	Diffusion coefficient for each species ($m^2 \cdot s^{-1}$)
n_i	Number density for each species ($A_L B_L, A_L^+, \ldots$)
e_0	Elementary charge (C)
Z_i	Valence of the ion, taken as 1
k	Boltzmann's constant
T	Absolute temperature (K)
φ	Electrical potential (V)
$\overrightarrow{u}$	Velocity vector ($mg \cdot s^{-1}$)

$$G_{B_L^-} = k_d^L n_0^L \tag{5}$$

$$R_{B_L^-} = k_r^L n_P^L n_N^L \tag{6}$$

where n_0^L, n_P^L, n_N^L are the neutral, positive and negative concentrations within the liquid, respectively. At the interface, a normal ionic flux density is imposed for the species B_L^- (Γ_{wall}^-) to allow the adsorption and desorption reactions:

$$\Gamma_{wall}^- = \left[\overbrace{k_{fn} n_N^L n_P^S}^{Adsorption} - \overbrace{k_{rn} n_N^{SL}}^{Desorption} \right] \tag{7}$$

where n_P^S and n_N^{SL} are the surface concentrations of the free (C_S) and occupied ($C_S B_L^-$) adsorption sites, respectively. Finally, all these equations are coupled to the Poisson's equation:

$$\nabla \cdot \left(\varepsilon_L \overrightarrow{E} \right) = e_0 \times \left(z_P n_P^L - z_N n_N^L \right) = \rho_L \tag{8}$$

where ε_L is the permittivity within the liquid, ρ_L is the space charge density. In the liquid region, the convection of the species are coupled to the Navier-Stokes equation. The simulation can be decomposed into two steps:

- **Static development of the EDL**: without fluid motion ($\overrightarrow{u} = 0$), the system reaches an equilibrium depending on different chemical kinetics.
- **Dynamic development of the EDL**: a flow is induced at the entry of the duct from the static equilibrium. The flow electrification process appears and the impact of the flow is studied.

2.3. Initial values and reaction rates of impurities

The initial concentration n_0 for the A_L^+ and B_L^- species in each region is estimated from the liquid conductivity as follows:

$$\sigma_0 = \frac{e_0^2}{kT} \left(D_P^L \left| z_P \right|^2 + D_N^L \left| z_N \right|^2 \right) \times n_0 \tag{9}$$

Thus, the different chemical reactions of ionized impurities in the liquid can be determined considering that the space charge density is initially zero and the ionization fraction is equal to 0.1. The initial data values are summarized in Table 1:

Table 1
Physical constants and initial values of reaction rates.

Constant	Symbol	Value
Liquid conductivity	σ_0	5×10^{-12} S·m^{-1}
Liquid permittivity	ε_L	$2.2\varepsilon_0$
Vacuum permittivity	ε_0	8.85×10^{-12} F·m^{-1}
Dynamic viscosity	ν	0.0014 kg·m^{-1}·s^{-1}
Liquid mass density	ρ_m	836.9 kg·m^{-3}
Ionic valence	z	1
Elementary charge	e_0	1.6×10^{-19} C
Ionic diffusion in liquid region	$D_{P,N,O}^L$	2.5×10^{-11} m^2·s^{-1}
Initial concentration (A_L^+, B_L^-)	n_o	1.58×10^{16} m^{-3}
Initial neutral ions concentration	n_{oi}	1.44×10^{18} m^{-3}
Recombination rate in the liquid	k_d^L	1.65×10^{-17} m^3·s^{-1}
Dissociation rate in the liquid	k_r^L	2.85×10^{-3} s^{-1}

Please cite this article in press as: P. Leblanc, et al., Impact of the laminar flow on the electrical double layer development, Journal of Electrostatics (2016), http://dx.doi.org/10.1016/j.elstat.2016.11.006

2.4. Evaluation of the adsorption/desorption rate from K_f

In order to calculate the adsorption and desorption chemical rates, the concentration of the preferential adsorption sites (n_P^{S0}) must be estimated. Cabaleiro [10], based on the Bourgeois work on a pressboard (dielectric solid) [11], assumed that (as an order of magnitude) $n_P^{S0} = 10^{25}$sites·m^{-3}. Thus, the inital surface concentration n_{P-surf}^{S0} can be estimated as follows:

$$n_{P-surf}^{S0} = n_P^{S0} \times \delta_0 \tag{10}$$

At the interface, previous work present a macroscopic models where a current density is given by the following equation [5]:

$$J_w = K_f \times (\rho_{wd} - \rho_w) \tag{11}$$

where ρ_w and ρ_{wd} are respectively the space charge density at the wall and the space charge density at the wall for a fully developed electrical double layer. Assuming that, at the equilibrium, all negative ions have reacted, Cabaleiro estimates the value of adsorption rate as follows [10]:

$$k_{fn} = \frac{2K_f}{n_{P-surf}^{S0}} \tag{12}$$

where δ_0 is the Debye length characterizing the EDL's diffuse layer's thickness [5]. Finally, after a parametric approach, Cabaleiro assumes that the number of occupied sites n_N^{SL} ($C_S B_L^-$) increases as the number of negative ions n_N^L (B_L^-) decreases. From this study, he determines that the ratio between n_N^L and n_N^S is equal to 0.01. The desorption rate can be expressed as:

$$k_{rn} = \frac{k_{fn}}{\delta_0} \times n_{P-surf}^{S0} \times 0.01 \tag{13}$$

In our study, two cases were considered to calculate the Adsorption/Desorption rate:

- K_f **is kept constant**: According to the classical theory, K_f is not impacted by the mean flow velocity and is equal to K_0.
- K_f **is variable**: The recent experimentations have shown that K_f might depended on the flow velocity. Thus, the simulation was carried out using the variation of K_f as a function of the mean flow velocity observed during an experimental campaign [9]:

$$K_f(U_m) = 1.43 \times 10^{-6} \times U_m + 1.67 \times 10^{-7} \tag{14}$$

The y-intercept ($K_0 = 1.67 \times 10^{-7}$ m·s^{-1}) represents the global rate of the chemical reactions without flow.

3. Geometry, mesh conditions and adimensionnal analysis

The simulation geometry is a rectangular duct of $100 \times 1 \times 0.0005$ mm^3 through which the liquid flows according to a laminar regime (Fig. 2). The mean flow velocity (U_m) is varied from 0.5m·s^{-1} to 5.5m·s^{-1}. For a symmetric condition in the y-direction, the calculation is made only on half of the duct.

Considering that, in our case, the characteristic length of the diffuse layer ($\delta_0 = 9.8689$ μm) is quite small compared to the duct's half height ($h = 1$ mm), the mesh was refined close to the interface where the gradients are stronger ($\Delta Z_{min} = 3.83 \times 10^{-7}$ m and $\Delta Z_{max} = 3.83 \times 10^{-5}$ m). Thus δ_0 is included in 22 cells and $3\delta_0$ in 42 cells.

Fig. 2 shows the different boundary conditions. At the interface of the solid (surface 4), the electric potential is zero (Dirichlet condition) and the normal ionic flux density for the species B_L^- is imposed by the non-homogeneous Neumann condition (Eq. (7)). Without a liquid flow, symmetry conditions are assumed on surfaces 1 and 3 (Homogeneous Neumann). When a liquid flow is induced, the entry condition (Poiseuille velocity profile) is imposed on surface 1 and the exit condition on surface 3 (Neumann homogeneous). On surface 2 and surfaces normal to the y-direction, a symmetry condition is applied (Homogeneous Neumann).

Finally all equations of the numerical model were adimensionalized according to the Vashy-Buckingham theorem. Four characteristic quantities were identified to carry out this non-dimensional operation. The first is the space charge density at the interface for a fully developed EDL ρ_{wd}^{ref} (0.0145 C·m^{-3}) when K_f is equal to K_0. This parameter is considered for different authors as an intrinsic parameter for one solid-liquid interface. The second one is the relaxation time constant ($\tau_r = \varepsilon_L/\sigma_0 = 3.9$ s). The third is the initial concentration of impurities (n_0). The fourth is a geometric term. For a rectangular duct, the half-height of the geometrical domain "h" is used. All the non-dimensional values were associated with the "*" symbol. This work focuses on the evolution of the space charge density near the interface (ρ_w) and the charge transported within the liquid (Q_L). Their associated non-dimensional parameters is expressed as follows:

$$\rho_w^* = \rho_w \left[\frac{1}{\rho_{wd}^{ref}}\right] \tag{15}$$

$$Q_L^* = Q_L \left[\frac{1}{h^3 \rho_{wd}^{ref}}\right] \tag{16}$$

4. Results and discussion

The non-dimensional space charge density at the wall (ρ_w^*) as a function of the contact duration ($\tau_c = U_m/L$) for different mean flow velocities is presented in Fig. 3. Regardless the mean flow velocity and the evolution of K_f^*, the space charge density is equal to zero at the entrance of the duct and increases progressively as a

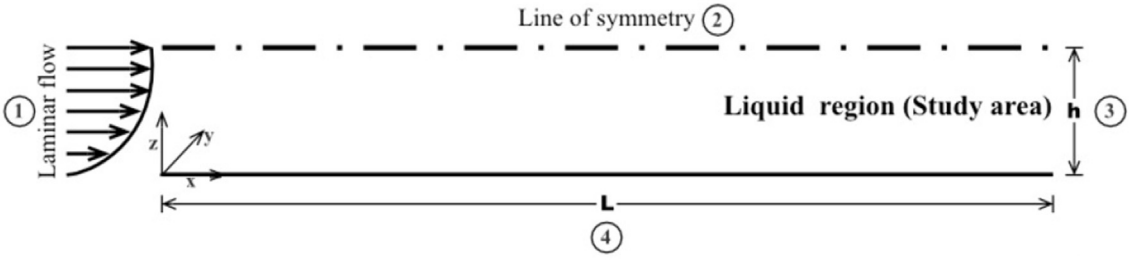

Fig. 2. Domain.

Please cite this article in press as: P. Leblanc, et al., Impact of the laminar flow on the electrical double layer development, Journal of Electrostatics (2016), http://dx.doi.org/10.1016/j.elstat.2016.11.006

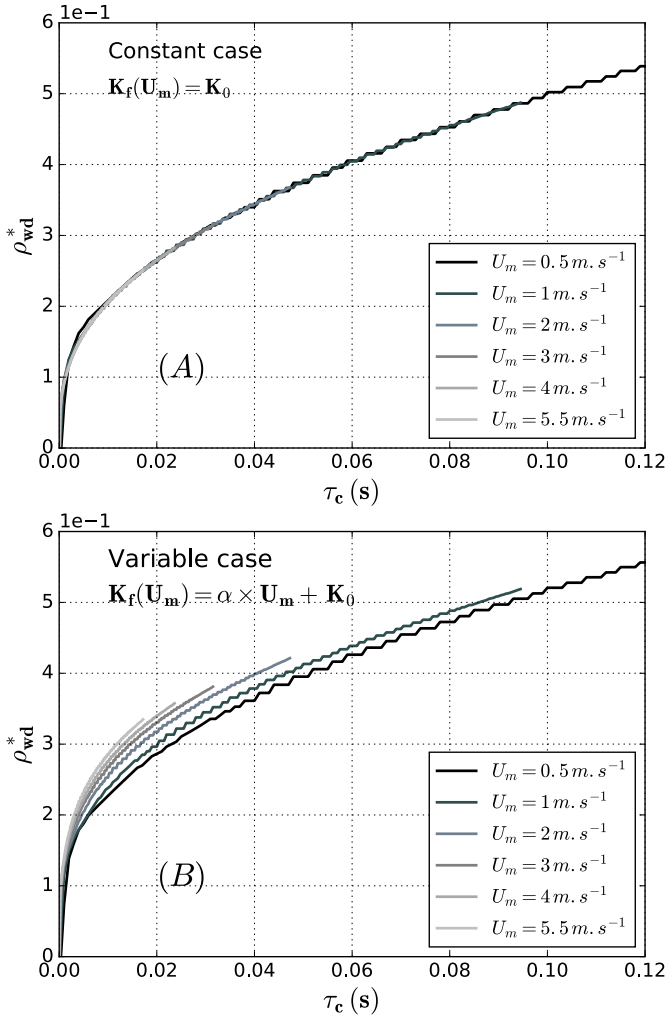

Fig. 3. Space charge density at the wall vs. contact duration.

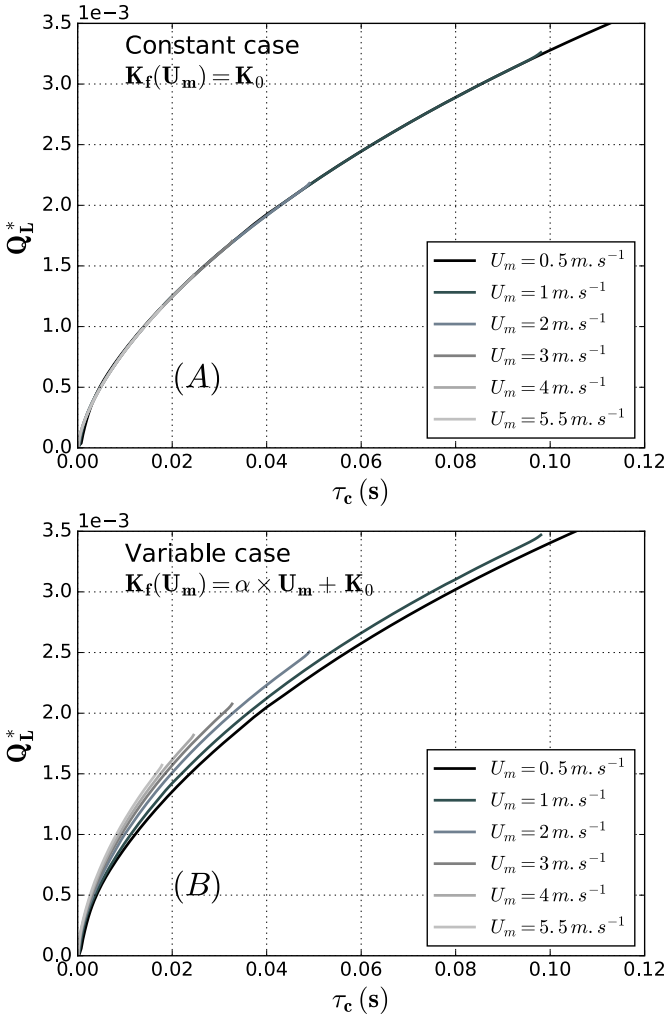

Fig. 4. Charge transported within the liquid vs. contact duration.

function of the contact duration. Furthermore, other simulations show that if the contact duration is sufficiently long, ρ^*_w reaches a maximum value $\rho^*_{wd} = 1$ and this regardless the value of K_f and U_m. In this case, the electrical double layer is considered fully developed. When the global rate of chemical reactions K_f is kept constant (Fig. 3-A), ρ^*_w adopts the same behavior regardless the mean flow velocity. The temporal dynamics of the EDL development remains constant and is in agreement with the classical theory.

However, when taking into account the linear variation for K_f (Fig. 3-B), recently highlighted from experiments, the dynamics of the EDL's development is impacted according to the mean flow velocity. Fig. 3 shows that the higher the magnitude of the mean flow velocity, the faster the development of the EDL. Indeed, the intensification of the global rate of chemical reactions allows decreasing the time required for the development of the space charge density. Concerning the non-dimensional transported charge Q^*_L as a function of the contact duration, the same observation could be carried out (Fig. 4). In the same way, the amount of transported charge remains identical whatever the magnitude of the mean flow velocity when K_f is constant (Fig. 4-A) whereas it increases in the case where K_f is variable (Fig. 4-B).

Fig. 5 plots the numerical and experimental non-dimensional transported charge as a function of the mean flow velocity for three different contact durations. Firstly, it is difficult to compare the magnitude of Q^*_L because the contact durations are much higher in the experimental case and also the numerical simulation was performed in a two-dimensional situation. Nonetheless, the trends can be compared. In both cases, the higher the contact duration, the higher the amount of transported charge. Regardless of the contact duration, Q^*_L increases progressively as a function of U_m. However, a slight difference can be observed. The variation of Q^*_L becomes faster when the contact duration increases in the experimental case whereas it remains identical in the numerical case. Even if the numerical simulation seems to be in rather good agreement, the model is not yet satisfactory. Clearly, it appears that the flow parameters has an impact on the EDL's development but it should not be simply reduced to a simple variation of chemical rate (e.g. k_{fn}, k_m).

In order to explain this behavior some authors [9] suggest that, increasing the velocity lead to increase the effective contact surface due to the porous nature of the solid (e.g pressboard). Nevertheless, this analysis seems to be insufficient in the case of a metallic solid. Other authors think that the variation of K_f is induced by the shearing stress [7,8]. Indeed, it is quite possible that the shearing stress modifies the different concentration of chemical species at the interface. Alternately, it can be assumed that the friction, induced at the interface, increases the local temperature. Thus, this variation suggests two important points:

Please cite this article in press as: P. Leblanc, et al., Impact of the laminar flow on the electrical double layer development, Journal of Electrostatics (2016), http://dx.doi.org/10.1016/j.elstat.2016.11.006

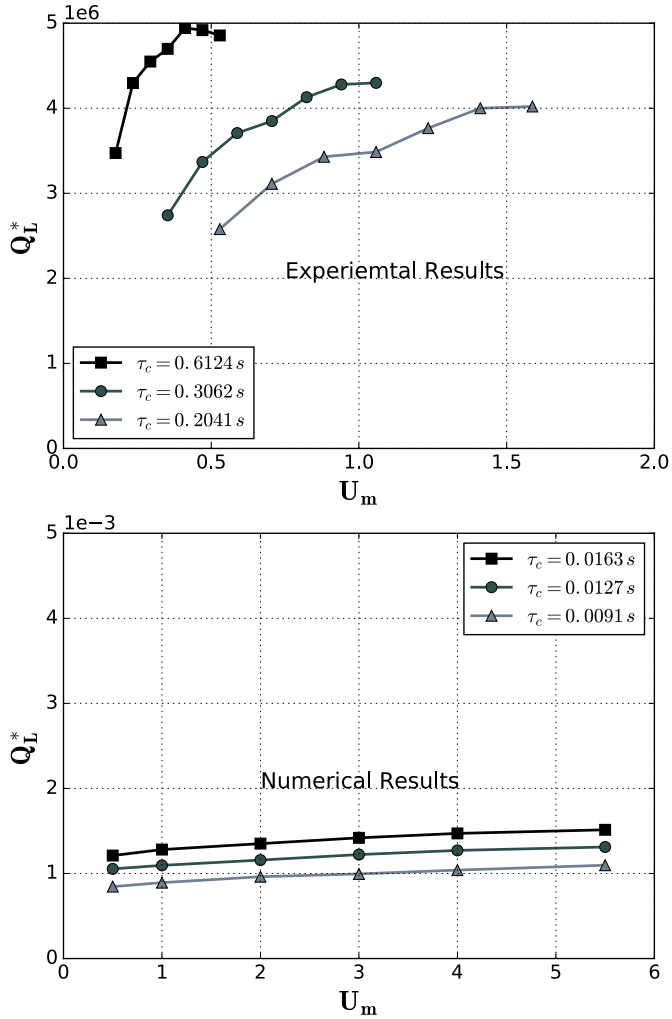

Fig. 5. Comparison between the experimental and numerical results of Q_L^* vs. U_m.

- an increase of the local temperature may modify the local ionic mobility, diffusivity, viscosity; hence a modification of the global rate of the chemical reaction.
- this modification is local and depends also on the position in the duct.

It appears necessary to take into account the local variation of the temperature and all the parameters (e.g mobility, diffusivity, viscosity) in a further model. Thus, it would be possible to simulate the flow electrification to deduce the variation of K_f and compare with the experimental campaign.

Acknowledgement

This work is supported by the French Government program — Investissements d'Avenir (LABEX INTERACTIFS, reference ANR-11 LABX-0017- 01).

Appendix A. Supplementary data

Supplementary data related to this article can be found at http://dx.doi.org/10.1016/j.elstat.2016.11.006.

References

[1] J. Gibbings, Electrostatics charging in the laminar flow in pipes of varying length, J. Electroanal. Chem. 25 (1970) 497–504.
[2] G. Touchard, Streaming current developed in laminar and turbulent flows trough a pipe, J. Electrost. 5 (1978) 463–476.
[3] T. Oommen, S. Lindgren, Statics electrification properties of transformers oil, IEEE Trans. Dielectr. Electr. Insul. 23 (1998) 123–128.
[4] H. Walmsley, G. Woodford, The generation of electric currents by the laminar flow of dielectric liquids, Journal of Physics 14.
[5] G. Touchard, T. Patzek, C. Radke, A physicochemical explanation for flow electrification in low-conductivity liquids in contact with a corroding wall, IEEE Transactions on Industry Applications 32.
[6] A.P. Washabaugh, M. Zhan, A chemical reaction-based boundary condition for flow electrification, IEEE Trans. Dielectr. Electr. Insul. 4 (1997) 688–709.
[7] O. Moreau, J. Cabaleiro, T. Paillat, G. Artana, G. Touchard, Influence of the wall shearing stress on flow electrification, in: Proc. International Symposium on Non Thermal Plasmas Electrical Discharges and Dielectric Material, Reunion Island, Oct. 2016.
[8] P. Leblanc, T. Paillat, J. Cabaleiro, G. Touchard, Flow electrification investigated under the effect of the wall shearing stress, in: Proc. 2016 Electrostatics Joint Conference, 2016.
[9] J. Cabaleiro, T. Paillat, G. Touchard, Flow electrification of dielectric liquids in insulating channels: Limits to the application of the classical wall current expression, Journal of Electrostatics.
[10] J. Cabaleiro, T. Paillat, O. Moreau, Modeling of static development and dynamic behavior of the electrical double layer at oil pressboard interface, in: Electrostatics Joint Conference, 2009.
[11] A. Bourgeois, Etude du phénomène d'élecrtrisation par écoulement sur les cartons des transformateurs de puissance, 2007. Ph.D. thesis, INP de Grenoble.